Global bifurcations at the onset of pulse self-replication

Baozeng Yue*
Department of Mechanics, School of Science, Beijing Institute of Technology, Beijing 100081, China
and Center for Mathematics and Computer Science, Amsterdam, Netherlands
(Received 17 January 2007; published 13 November 2007)

In this work, we carried out an extensive numerical exploration of the delicate global dynamics of pulse self-replication and analyzed the stability of singular homoclinic stationary solutions and their bifurcations in the one-dimensional Gray-Scott model. This stability analysis has several implications for understanding the recently discovered phenomena of self-replicating pulses. The solutions of the ordinary differential equation are organized around a codimension-2 global bifurcation from which two or N branches of homoclinic orbits originate, corresponding to solitary pulse solutions in the partial differential equation. A careful analysis of the bifurcation scenarios in the global bifurcation diagram suggests that the dynamics of the self-replicating system are related to a hierarchy structure of folding bifurcation branches in parameter space. The numerical simulation suggests that the Bogdanov-Takens points, together with the presence of critical points emanating from a particular codimension-2 homoclinic orbit, play a central role for the global bifurcation of periodic orbits, the homoclinic solutions, and the complex chaotic dynamics. The numerical simulation also reveals the existence of a modulating two-pulse or multipulse, which accompanies the procedure of pulse self-replication in reaction-diffusion systems.

DOI: 10.1103/PhysRevE.76.056209 PACS number(s): 82.40.Bj, 82.40.Ck, 02.30.Jr

I. INTRODUCTION

Global or homoclinic bifurcations of dynamical systems are important in applications for a number of reasons [1–32]. First, homoclinic orbits may be "organizing centers" for dynamics in their neighborhood. From their existence one may, under certain conditions, infer the existence of chaos nearby or the bifurcation behavior of periodic orbits. Second, if the dynamical system arises as the traveling wave equation for a partial differential equation or system, then homoclinic solutions of it describe solitary waves, which are of importance in many fields [1]. One example is reaction-diffusion systems, which are multicomponent models involving diffusion and nonlinear interaction among the components. Such systems are commonplace in many areas of physics, chemistry, and biology. They are used as a model for such diverse phenomena as cell differentiation, chemical reaction, propagation of flame fronts, laser interference, and sea shell patterns. The modern theory of pattern formation begins with the seminal 1952 paper by Turing. This theory used linear analysis to determine threshold conditions for the instability of spatially homogeneous equilibria of general two-component reaction-diffusion systems. However, Turing's method is limited to patterns that are near-homogeneous in space. As such, it fails to predict the stability and dynamics of spike-type solutions corresponding to homoclinic orbits, which are ubiquitous in many reaction-diffusion systems [2–10]. The stability of spike-type solutions—where Turing's method is not applicable—is the main topic of this paper.

The Gray-Scott model is referred to as an activator-substrate system, which exhibits a variety of new patterns, including self-replicating spots that develop into a variety of asymptotic states in two dimensions, as well as pulses that self-replicate in one dimension [2–5]. Here, the chemical u can be interpreted as a substrate depleted by v. The long-range inhibition here is due to depletion of u. The activation is due to the presence of the source term in the equation for u. There are some cornerstones in the development of the Gray-Scott model. The numerical and laboratory experiments by Pearson *et al.* have spurred the development of new analytical techniques to understand these patterns [3–10]. Some analytical results on spike-type solutions were derived by Doelman and co-workers in a series of papers starting with [6]. Their theory analytically explains certain stability properties of spike-type solutions in the one-dimensional Gray-Scott model. Several interesting analytical works have also appeared: for instance, using formal matched asymptotic analysis, Reynolds *et al.* [4,5] have constructed a single-spot solution and studied its stability, which is closely related to the replicating phenomenon; a rigorous analysis concerning the existence and stability of a steady single pulse as well as nonexistence of traveling pulses has been done by Doelman *et al.* [6–8]. Although these works are very suggestive, very little is known about the mechanism that drives the replication dynamics itself. Thus, the aim of this paper is to present a key mechanism for the self-replicating dynamics for the Gray-Scott model.

Two-pulse patterns play a fundamental role in the numerical simulation of pulse replication in one-dimensional problems. In order to understand this phenomenon, it is necessary to study the stability of solutions consisting of a pair of pulses, in which the pulses move apart from each other [9]. In this study, we not only carry out an existence and stability analysis for two-pulse patterns in the one-dimensional Gray-Scott model, but also present the modulating multipulse, which can be used to describe the stability and replication of the initial stationary multipulse patterns. We study, mainly numerically, the two-pulse and multipulse pattern dynamics in the Gray-Scott model. The numerical simulation reveals the geometrically hierarchical structure of the bifurcation

*bzyue@sohu.com

diagram in parameter space. Simulation results in this paper partially confirm the analytical conclusions about the bifurcation scenarios [10]. It is shown that Bogdanov-Takens (BT) points play a central role for the global bifurcation of periodic orbits and homoclinic orbits. Intuitively, BT points serve as a source of homoclinic branches, in two parameters, in very much the same way as Hopf bifurcations, in one-parameter families, serve as a source of branches of periodic orbits. In fact, the similarity between periodic and homoclinic bifurcations will be more than a superficial analogy. Homoclinic orbits can be viewed as limits of nearby periodic orbits. Numerical results confirm the existence of periodic and homoclinic orbits cascading to a saddle center at isolated parameter values, which gives rise to multiplicity and shift dynamics.

In this paper, we confine ourselves to the one-dimensional case and mainly investigate the apparent loss of stability of one-pulse and multipulse solutions and the transition to shift dynamics in the excitable regime. The rest of the paper is outlined as follows. Section II gives a derived scaled Gray-Scott model and briefly analyzes the stability of the stationary solutions. Section III contains the numerical procedure used in the present simulation and the global bifurcation diagram of two-pulse and multipulse solutions obtained by the present numerical procedure. Section IV presents the numerical results, including pulse self-replication, homoclinic orbit cascade, and modulated two and multiple pulses. It also presents (a) a height instability where the spike height oscillates and (b) an oscillatory drift instability where the center of the spike exhibits spatially periodic motion. The final section (Sec. V) provides insight into the central role of the global bifurcation, provides a qualitative comparison between the analytic results and those obtained from numerical simulation, and also gives some concluding remarks.

All the computations in this paper are performed using the continuation software AUTO 2000.

II. MODEL EQUATIONS

In this paper, we carry out an extensive numerical global bifurcation study in the one-dimensional Gray-Scott model [11] (see also the references in [10,12,13] for the derivation and early studies of this model):

$$\frac{\partial u}{\partial t} = \frac{\partial^2 u}{\partial x^2} - uv^2 + A(1-u), \tag{1}$$

$$\frac{\partial v}{\partial t} = D\frac{\partial^2 v}{\partial x^2} + uv^2 - Bv. \tag{2}$$

For all positive values of the parameters A, B, and D, the background homogeneous state $(u \equiv 1, v \equiv 0)$ is stable. The homoclinic orbits or pulse solutions considered in this paper are asymptotic to this basic state as $x \to \pm\infty$. The pulses correspond to excursions of the v components away from the $v \equiv 0$ background state on narrow intervals; the u component varies significantly outside these regions and is in general not close to $u \equiv 1$ in between the v pulses. For stationary solutions of Eqs. (1) and (2), we further reduce the number of parameters by introducing new independent and dependent variables and constants:

$$\tilde{x} = Bx,$$

$$\tilde{u}(\tilde{x}) = u(x),$$

$$\tilde{v}(\tilde{x}) = \frac{1}{B}v(x),$$

$$\lambda = \frac{A}{B^2},$$

$$\gamma = BD.$$

When we drop the tildes, this yields the following system of two coupled ordinary differential equations:

$$\frac{\partial^2 u}{\partial x^2} - uv^2 + \lambda(1-u) = 0, \tag{3}$$

$$\gamma\frac{\partial^2 v}{\partial x^2} + uv^2 - v = 0. \tag{4}$$

Equations (3) and (4) can be written as a system of four first-order differential equations,

$$u' = p, \tag{5}$$

$$p' = uv^2 - \lambda(1-u), \tag{6}$$

$$v' = q, \tag{7}$$

$$q' = \frac{1}{\gamma}(v - uv^2), \tag{8}$$

where the prime denotes d/dx. Constant stationary solutions or fixed points satisfy the following equations:

$$p = 0, \tag{9}$$

$$uv^2 - \lambda(1-u) = 0, \tag{10}$$

$$q = 0, \tag{11}$$

$$\frac{1}{\gamma}(v - uv^2) = 0. \tag{12}$$

We obtain three fixed points S_i, $(i=1,2,3)$, i.e.,

$$S_1 = \left(\frac{1-\sqrt{1-4/\lambda}}{2}, 0, \frac{\lambda(1+\sqrt{1-4/\lambda})}{2}, 0\right),$$

$$S_2 = \left(\frac{1+\sqrt{1-4/\lambda}}{2}, 0, \frac{\lambda(1-\sqrt{1-4/\lambda})}{2}, 0\right),$$

$$S_3 = (1,0,0,0).$$

Numerical experiments confirm that the fixed point S_3 is of saddle type, and, depending on the parameter region, S_1 and

S_2 might become saddle type, saddle-center type, focus type, saddle-focus type, double-Hopf type, BT type, or Bogdanov-Takens-Hopf type points. In the next section, we focus on the critical point S_1 to study the global bifurcation dynamics at the onset of pulse self-replication.

III. HIERARCHY STRUCTURE OF BIFURCATION DIAGRAM

Since the appearance of homoclinic orbits corresponds to a global bifurcation, it is usually hard to analytically prove their existence in example systems. The best one can normally hope for is to prove their existence near certain singularities. One way to do this is by locating a codimension-2 local bifurcation such as a BT point, i.e., an equilibrium with eigenvalues $\mu_{1,2}=0$ which is the origin of loci of homoclinic orbits in certain cases. To begin with, suppose that only one active parameter is chosen, so that there are isolated parameter values at which regular homoclinic orbits occur. These isolated parameter values, together with approximations to the homoclinic orbits, may be sought numerically by continuing periodic solutions to large periods or by using the shooting method. For clarity, we study the global bifurcation phenomena that exist for $\lambda > 4$, and $\gamma \in [0, 1/4]$. These are the ranges of parameter values for which there exist patterns in the form of pulses and kinks [12]. The numerical simulations in this paper reveal the possibility of resonant homoclinic doubling orbits and doubling spatially periodic orbits for that range of parameter values. Hence, the corresponding bifurcation diagram consists of (1) a complicated structure involving a fan of infinitely many n-periodic and n-homoclinic orbits for arbitrary n and (2) a region with horseshoe dynamics. This computation starts from an equilibrium at $S_1=(0.2764, 0.0, 3.6180, 0.0)$, which exists for $\lambda = 5.0$ and $\gamma=0.01$. This equilibrium is not the one corresponding to the homoclinic orbit, but it is an equilibrium with imaginary eigenvalues, which we can follow until it reaches a Hopf bifurcation.

A spatially periodic orbit emanates from this Hopf bifurcation and can be followed to the homoclinic orbit. In all the following computations, the spatial variable is rescaled so that the period becomes unity. To start the continuation of loci of homoclinic orbits, initial approximations are needed. Various strategies for doing this are possible as described above. In the present computations, the initial approximations for homoclinic orbits are obtained by following periodic solutions, which typically bifurcate from certain Hopf bifurcation points, to large period (sometimes we need to perform a time shift on the data from a periodic orbit). The codimension-2 homoclinic bifurcation points are detected along the primary branch by locating zeros of certain test functions. The issue of defining these test functions is actually twofold. First, consider the primary codimension-1 homoclinic orbits to the original problem on the infinite interval. A test function for a certain codimension-2 homoclinic bifurcation is a smooth function defined along the primary branch so that its regular zeros correspond to the occurrence of the bifurcations. Afterward, we need to define a test function for the truncated boundary-value problem on the finite interval. In the simplest cases, test functions are obtainable from eigenvalues of the equilibrium. In most cases of the following computations we survey the occurrence of neutral (resonant) saddle where fold (saddle-node) bifurcations of spatially periodic orbits or resonant homoclinic doubling orbits will occur.

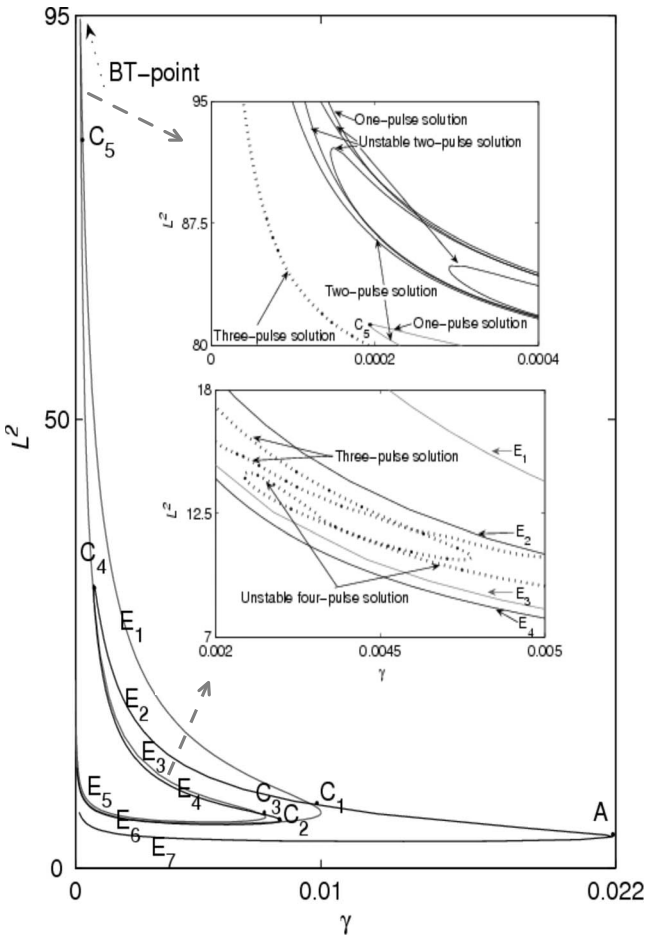

FIG. 1. Hierarchy structure of the global bifurcation. E_i $(i=1,\ldots,7)$ are used to label curves. C_i $(i=1,\ldots,5)$ and A, are used to label the points with the following coordinates (in order): C_1 (0.0123,6.5049), C_2 (0.0084,5.2592), C_3 (0.0078,5.663), C_4 (0.0008,31.5127), C_5 (0.0002,94.5642), A (0.0219,3.3444).

Figure 1 depicts the global bifurcation diagram, which was computed using the standard local bifurcation features of AUTO 2000 and HOMCONT software [14]. The vertical axis denotes the L^2 norm of solutions $(u(s), p(s), v(s), q(s))$ and the horizontal one is the bifurcation parameter γ. We do not mark the BT point exactly but can infer its existence from the bifurcation diagrams in its neighborhood. Curves labeled E_1, E_5, and E_7 are the loci of one-pulse solutions. Curves labeled E_6, E_3, and E_4 are the loci of two-pulse solutions. Curves labeled E_2, C_4C_5, and AC_1 are the loci of spatial period-2 solutions.

Figure 1 also contains magnification of its two parts, i.e., the magnifications of the left top corner and of the left bottom corner. From the magnification of the left top corner, we have found one-pulse and two-pulse solutions as well as an unstable two-pulse solution, which oscillates in its ampli-

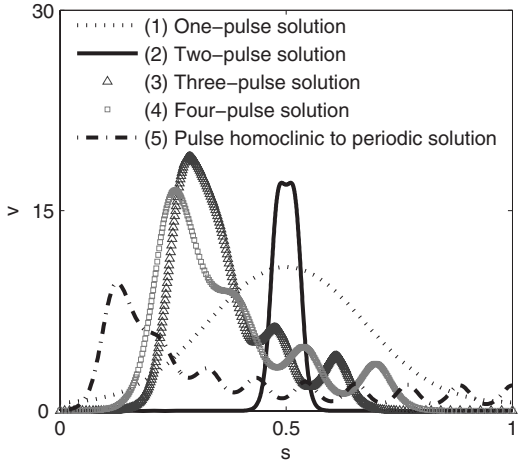

FIG. 2. Initial solutions produced from the continuation of the domain length.

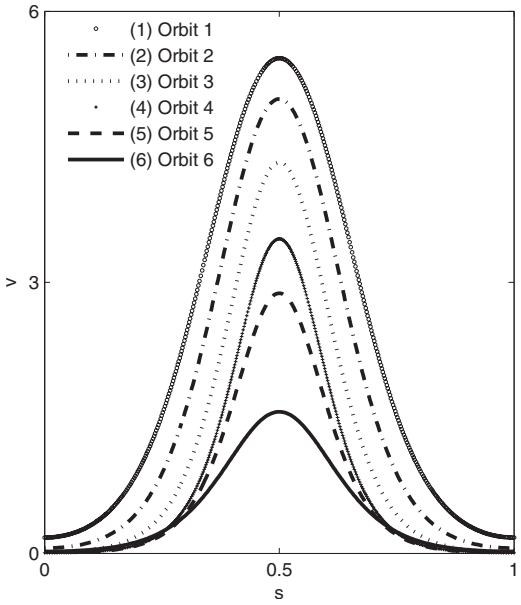

FIG. 3. Stable one-pulse solutions produced from the continuation of a one-pulse solution.

tude, shifts its location, and exhibits a self-replication symptom over a range of parameter values. The magnified picture of the left bottom corner shows a stable three-pulse, an unstable three-pulse, and an unstable four-pulse. In tracing the loci of homoclinic orbits, we check different neutral (resonant) saddle-focus points with different initial parameter data. (If all the leading eigenvalues are real, the equilibrium is termed a real saddle or saddle for short; if all the leading eigenvalues are complex, the equilibrium is termed focus focus or bifocus. In all other cases the equilibrium is called a saddle focus.) Generally, there are several infinite series of codimension-1 bifurcation curves that accumulate in a complicated manner near the fold bifurcation line (shown by numerical experiments to be the vertical axis in Fig. 1) which passes through the BT point. More precisely, there is a countable number of spatially periodic curves corresponding to fold bifurcations of cycles with increasing number of rotations near the saddle-focus point. The other infinite series of codimension-1 bifurcation curves are composed of double homoclinic curves, an orbit that makes two big excursions near the primary homoclinic orbit before returning to equilibrium. The entire bifurcation scenarios are even more involved since there is a countable set of various triple homoclinic bifurcation curves located between each pair of double homoclinic curves. As such, we can conjecture a whole hierarchical structure of a global bifurcation diagram, which looks like a millefeuille.

IV. NUMERICAL SIMULATIONS

A recent version of the AUTO software includes a library of routines called HOMCONT that allows the user to track homoclinic and heteroclinic orbits [14]. The hardest part of computing a branch of homoclinic orbits is finding a starting point. Here we consider a differential equation

$$y' = f(y,\alpha), \tag{13}$$

where $y=(u,p,v,q)^T$ and α is a free parameter. Homoclinic orbits are codimension-1 trajectories; they are expected to occur only at a particular value of a parameter, say, $\alpha=0$. We suppose we have computed an approximate homoclinic orbit to the fixed point y_e which has an n_s-dimensional stable manifold and an n_u-dimensional unstable manifold. We assume $n_s+n_u=n$, where n is the dimension of the system. The way that a homoclinic orbit is computed is by approximating it on a finite interval; say $[0,L]$. We rescale the independent variable x by $x=Ls$. We want to start along the unstable manifold and end on the stable manifold. Let L_u be the projection onto the unstable subspace of the linearization of f about the fixed point and let L_s be the projection onto the stable space. After this, we want to solve the following system:

$$\frac{dy}{ds} = Lf(y,\alpha), \tag{14}$$

$$\frac{dy_e}{ds} = 0, \tag{15}$$

$$f[y_e(0)] = 0, \tag{16}$$

$$L_s[y(0) - y_e(0)] = 0, \tag{17}$$

$$L_u[y(1) - y_e(0)] = 0, \tag{18}$$

where y_e represents the equilibrium. Since $y(s)$ can be translated freely in the spatial domain, that is, if $y(s)$ is a spatial periodic solution then so is $y(s+\sigma)$, for any σ, a phase condition is needed. Suppose that we have computed a homoclinic orbit $\hat{y}$. Then we want to minimize the least-squares difference between the new solution and the old solution to set the phase:

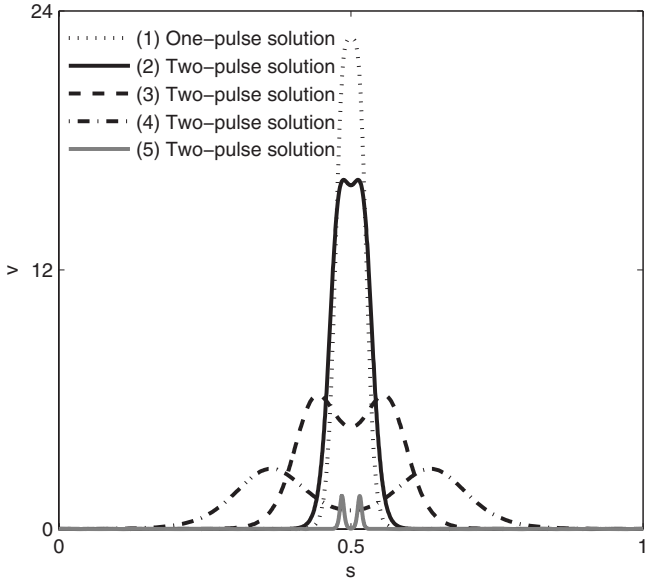

FIG. 4. Stable two-pulse solutions produced from the continuation of a one-pulse solution.

$$D(\sigma) \equiv \int_0^1 \|y(s+\sigma) - \hat{y}(s)\|^2 ds = 0. \tag{19}$$

The optical solution $y(s+\hat{\sigma})$ satisfies the necessary condition $dD/d\sigma=0$, that is,

$$\int_0^1 [y(s+\hat{\sigma}) - \hat{y}(s)]y'(s+\hat{\sigma})ds = 0. \tag{20}$$

Writing $y(s) \equiv y(s+\hat{\sigma})$ leads to the following integral condition (or phase condition):

$$\int_0^1 y'(s)[y(s) - \hat{y}(s)]ds = 0. \tag{21}$$

This is one more condition that compensates for the additional free parameter.

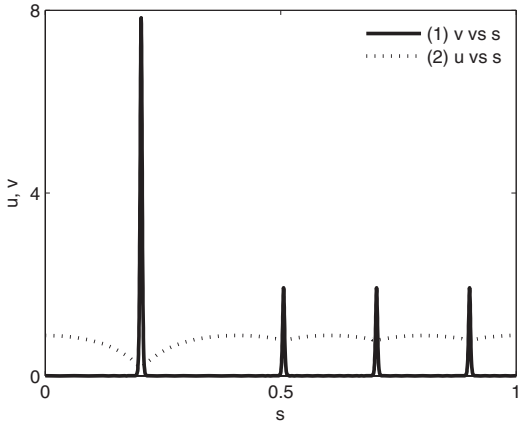

FIG. 5. Four-pulse solution produced from the continuation of a two-pulse solution.

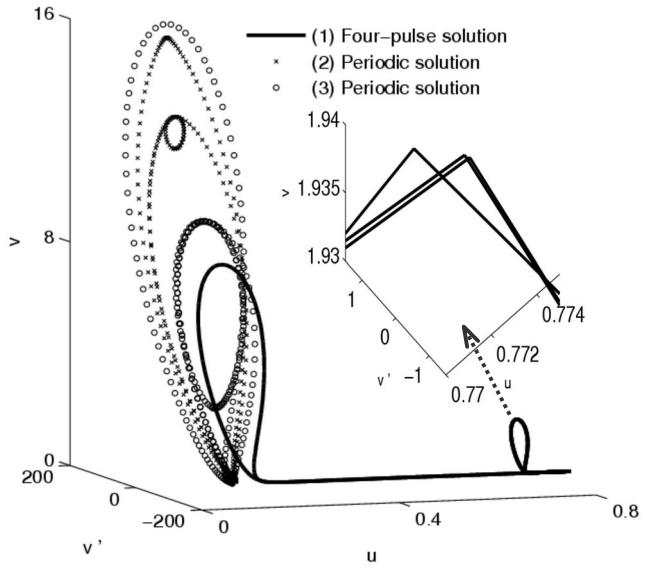

FIG. 6. Phase diagram of four-pulse solution and spatially periodic orbits. Parameters corresponding to the orbits are as follows: $\lambda=4.348\,015$ and $\gamma=3.572\,798\times10^{-5}$ for orbit 1; $\lambda=5.142\,309$ and $\gamma=4.036\,950\times10^{-5}$ for orbit 2; $\lambda=7.284\,555$ and $\gamma=4.187\,064\times10^{-5}$ for orbit 3.

The mainly numerical simulation results are presented in Figs. 2–9. Figure 2 is obtained by using the domain length L as the continuation parameter. At this stage, multimodel solutions initially approximating pulse solutions were found. It can also be observed from Fig. 2 that the system possesses a kind of solution that is homoclinic to a spatially periodic orbit (this kind of solution will be an interesting topic for future work). Taking the approximate solutions obtained at this stage as the initial data, we can further advance the con-

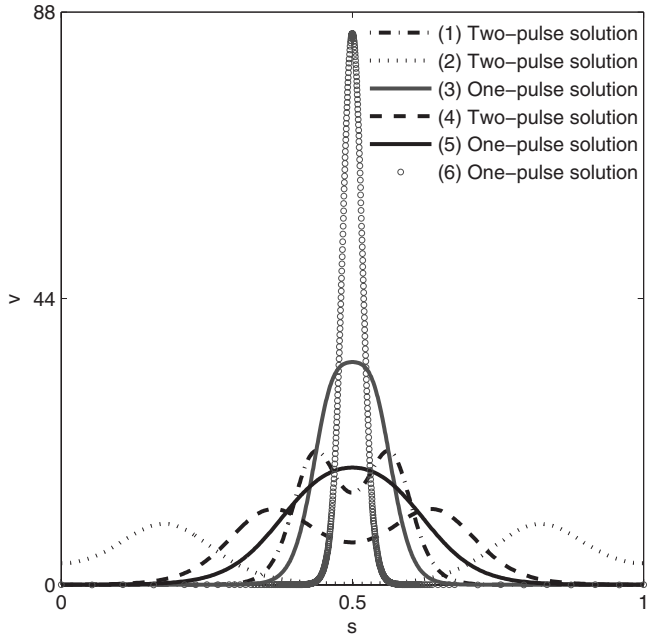

FIG. 7. One- and two-spike modulated pulses produced from the continuation of a one-pulse solution.

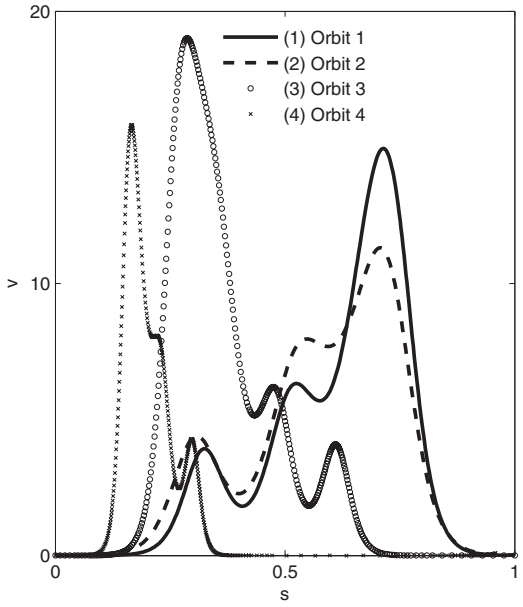

FIG. 8. Three-spike modulated pulses produced from the continuation of a two-pulse solution.

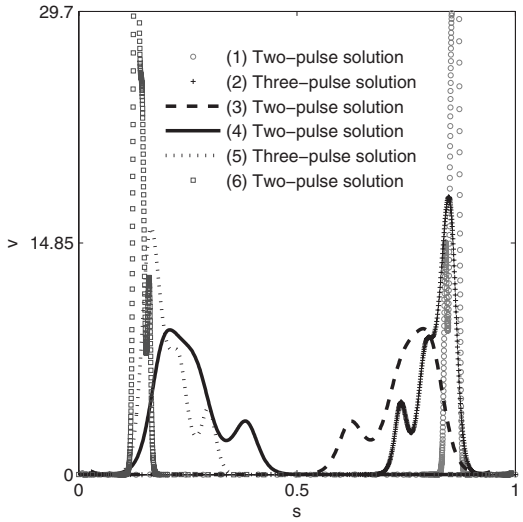

FIG. 9. Two- and three-spike modulated pulses produced from the continuation of a two-pulse solution.

tinuation in codimension 1 or codimension 2. The stable homoclinic solutions are obtained by tracing, in parameter space, the loci of solutions obtained at the first stage of the continuation.

Figure 3 is obtained by codimension-1 continuation, where a number of stable one-homoclinic orbits are depicted corresponding to a series of parameters. Figure 4 presents stable two-homoclinic solutions, which are also created by codimension-1 continuation. A replicating phenomenon, i.e., where one pulse splits into two pulses, is obvious in Fig. 4. In the same way, Fig. 5 is obtained by following a two-homoclinic orbit in parameter space, while, in this situation, the continuation is carried out in codimension-2, starting off at a fold bifurcation point.

Figure 6 is the phase diagram of a four-homoclinic orbit corresponding to Fig. 5. In addition, there are two spatially periodic orbits included in Fig. 6 for visual comparison between homoclinic orbits and periodic orbits. It is observed that the so-called resonant homoclinic orbit bifurcation is accompanied by periodic orbit doubling. The similarity between periodic and homoclinic bifurcation will, in fact, be more than a superficial analogy. Viewing homoclinic orbits as limits of nearby periodic orbits will serve in many cases as the basic technical tool for global continuation. The right three small-amplitude excursions in Fig. 6 are located so close in phase space that they can hardly be distinguished visually from each other. Magnification of the top part of these small-amplitude excursions in Fig. 6 clearly shows three pulses corresponding to these excursions. Figure 6 also clearly shows how the double homoclinic orbit emanated from doubling periodic orbits.

Figure 7 shows an undercrowding instability or replication. In the presence of such instability, successive spike replication is observed, until a certain threshold number of spikes is exceeded. Figure 8 reveals an asymmetric three-homoclinic orbit shift oscillation. Figure 9 shows an unstable two-homoclinic orbit switched from two-pulse to three-pulse over a range of parameter values. From Figs. 7–9 we clearly observe an oscillatory height instability whereby the spike height oscillates as the parameter γ is varied over a range of its values. An oscillatory drift instability was also discovered in numerical simulations presented here (particularly in Figs. 7–9), where the center of the spike oscillates periodically in space. The numerical simulations indicate that when the spike center approaches the edge of the domain, it triggers an oscillatory profile instability, so that oscillations in spike height are observed at that point. Tables I and II show a pair of parameters λ and γ corresponding to the replications in Figs. 7 and 9, respectively.

V. CONCLUDING REMARKS

In this work, we discussed the basic process of self-replication, typically from a single pulse. The mechanism proposed here seems rather universal and has the potential of becoming a general framework to explain self-replication patterns. In this study, we confirmed that the Gray-Scott model has a rich variety of global bifurcation phenomena or

TABLE I. Parameters corresponding to the replication in Fig. 7.

Orbit	1	2	3	4	5	6
λ	4.851740	5.050192	5.692233	5.536860	5.946925	4.198855
γ	1.667643×10^{-4}	9.216931×10^{-4}	1.249755×10^{-4}	6.703408×10^{-4}	7.502311×10^{-4}	2.574930×10^{-5}

TABLE II. Parameters corresponding to the replication in Fig. 9.

Orbit	1	2	3	4	5	6
λ	4.218774	4.365061	4.252033	4.388382	4.497610	4.432856
γ	1.992570×10^{-3}	4.527053×10^{-3}	1.095857×10^{-2}	9.232236×10^{-4}	6.355146×10^{-4}	2.15076×10^{-4}

patterns. These types of patterns only exist in a restricted "horn" area in parameter space, and the whole global bifurcation diagram is an intricate hierarchical structure. Such a skeleton of coherent structures demonstrates its organizing center from which emanates an infinite number of fold and flip (period-doubling) bifurcations involving periodic orbits corresponding to a double homoclinic orbit. The numerical simulations also confirmed a finite number of existing modulated n-homoclinic orbits in the process of global bifurcation. Full numerical simulations indicate that the Hopf bifurcation corresponding to the oscillatory profile instability is subcritical, and therefore leads to the eventual collapse of the spike. It is confirmed that a kind of replication from $2n$ pulses to $2n+1$ pulses is extremely unstable and persists over only a small range of parameter values. This numerical result is in accordance with the analytical conclusion of Doelman *et al.* [10].

ACKNOWLEDGMENTS

I wish to express my gratitude to the referees for their useful comments and suggestions. I am also indebted to Professor Arjen Doelman from CWI (Centrum voor Wiskunde en Informatica, Amsterdam, Netherlands) for his hospitality. This research was supported by the China Scholarship Council and the Natural Science Foundation of China (Grants No. 10572022 and No. 10772026).

[1] S. Smale, Bull. Am. Math. Soc. **73**, 747 (1967).
[2] P. Gray and S. K. Scott, Chem. Eng. Sci. **39**, 1087 (1984).
[3] J. E. Pearson, Science **216**, 189 (1993).
[4] W. N. Reynolds, J. E. Pearson, and S. Ponce-Dawson, Phys. Rev. Lett. **72**, 2797 (1994).
[5] W. N. Reynolds, J. E. Pearson, and S. Ponce-Dawson, Phys. Rev. E **56**, 185 (1997).
[6] A. Doelman, R. A. Gardner, and T. J. Kaper, Physica D **122**, 1 (1998).
[7] A. Doelman, T. J. Kaper, and P. Zegeling, Nonlinearity **10**, 523 (1997).
[8] A. Doelman and T. J. Kaper, SIAM J. Appl. Dyn. Syst. **2**, 53 (2003).
[9] A. Doelman, W. Eckhaus, and T. J. Kaper, SIAM J. Appl. Math. **61**, 2036 (2001).
[10] A. Doelman, T. J. Kaper, and L. A. Peletier, J. Differ. Equations **231**, 359 (2006).
[11] Y. Nishiura and D. Ueyama, Physica D **130**, 73 (1999).
[12] J. K. Hale, L. A. Peletier, and W. C. Troy, SIAM J. Appl. Math. **61**, 102 (2000).
[13] Y. Nishiura and D. Ueyama, Physica D **150**, 137 (2001).
[14] E. J. Doedel *et al.*, computer code AUTO 2000, ftp://ftp.cs.concordia.ca/pub/doedel/auto
[15] T. Kolokolnikov, M. J. Ward, and J. Wei, Physica D **202**, 258 (2005).
[16] T. Kolokolnikov, M. J. Ward, and J. Wei, Stud. Appl. Math. **115**, 21 (2005).
[17] D. Iron, M. J. Ward, and J. Wei, Physica D **150**, 25 (2001).
[18] A. Doelman and P. Holmes, Philos. Trans. R. Soc. London, Ser. A **354**, 845 (1996).
[19] A. R. Champneys and Y. A. Kuznetsov, Int. J. Bifurcation Chaos Appl. Sci. Eng. **4**, 795 (1994).
[20] A. R. Champneys and Y. A. Kuznetsov, Report No. AM-R9308, Center for Mathematics and Computer Science, Amsterdam, The Netherlands, 1993 (unpublished).
[21] S. Wiggins, *Global Bifurcations and Chaos—Analytical Methods* (Springer-Verlag, New York, 1998).
[22] J. Billingham and D. J. Needham, Philos. Trans. R. Soc. London, Ser. A **334**, 1 (1991).
[23] J. Billingham and D. J. Needham, Philos. Trans. R. Soc. London, Ser. A **336**, 497 (1991).
[24] M. del Pino, M. Komalczyk, and X. Chen, Commun. Contemp. Math. **3**, 419 (2001).
[25] K. Kanneko, Physica D **34**, 1 (1989).
[26] A. Doelman, R. A. Gardner, and T. J. Kapper, Indiana Univ. Math. J. **50**, 443 (2001).
[27] H. van der Ploeg andA. Doelman, Indiana Univ. Math. J. **54**, 1219 (2005).
[28] H. Takagi and K. Kaneko, Int. J. Bifurcation Chaos Appl. Sci. Eng. **12**, 2579 (2002).
[29] A. Doelman and H. V. D. Ploeg, SIAM J. Appl. Dyn. Syst. **1**, 65 (2002).
[30] Y. Kuznetsov, *Elements of Applied Bifurcation Theory*, Applied Mathematical Sciences Vol. 112 (Springer-Verlag, New York, 1995).
[31] C. B. Muratov and V. V. Osipov, J. Phys. A **33**, 8893 (2000).
[32] C. B. Muratov and V. V. Osipov, SIAM J. Appl. Math. **62**, 1463 (2002).